Interfaces and Free Boundaries **4**, (2002) 395–421

Motion by curvature of a three-dimensional filament: similarity solutions

G. RICHARDSON† AND J. R. KING
Division of Theoretical Mechanics, School of Mathematical Sciences, University of Nottingham, Nottingham, NG7 2RD, UK

[Received 2 July 2001 and in revised form 16 May 2002]

We systematically classify and investigate fully three-dimensional similarity solutions to a system of equations describing the motion of a filament moving in the direction of its principal normal with velocity proportional to its curvature, $\boldsymbol{v} = \kappa \boldsymbol{n}$, where $\boldsymbol{n}$ is the principal normal and κ the curvature of the filament. Such formulations are relevant to superconducting vortices and disclinations.

Keywords: Motion by curvature

1. Introduction

There are many physical systems which exhibit line singularities [3]. These are characterized by a singularity in a certain quantity which occurs along a curve in three-space. So, for instance, a disclination in a nematic liquid crystal is a curve along which the director, a vector field which gives the preferred direction for molecular alignment, is multivalued. Other examples of line singularities are the superconducting vortex, the superfluid vortex (which is found in liquid helium) and the dislocation (which is a misalignment of a crystal lattice). In many scenarios the behaviour of these systems is primarily governed by the presence of these singularities and it is possible to derive linear field equations with singularities along curves, corresponding to the positions of the line singularities, which couple to a law of motion for these curves. In the case of the superconducting vortex, for example, the vortex law of motion

$$\boldsymbol{v} = \kappa \boldsymbol{n} + (\nabla \wedge \boldsymbol{B}) \wedge \boldsymbol{t}, \tag{1}$$

couples to a linear field equation for the magnetic field $\boldsymbol{B}$ [6]. Here $\boldsymbol{v}$ is the velocity of the vortex, κ its curvature, $\boldsymbol{t}$ its tangent and $\boldsymbol{n}$ its principal normal. The first term in this velocity law is a self-induced term while the second term can be thought of as arising from the presence of other vortices and boundaries. Situations inevitably arise in which the first term dominates so that the motion can be approximated by

$$\boldsymbol{v} = \kappa \boldsymbol{n}, \tag{2}$$

for example when vortices are well separated. It is conjectured that line disclinations in certain nematic liquid crystal also have this form for the self-induced velocity. † In a certain limit the

†Corresponding author. Email: giles.richardson@maths.nottingham.ac.uk

†A two-dimensional velocity law has been derived for a certain class of disclination in [14], which is such as to suggest that the corresponding three-dimensional law contains a self-induced term similar to equation (1).

dynamics of scroll waves, which occur in excitable media, also obey equation (2) [8]. In contrast to these systems the leading-order self-induced velocity of the superfluid vortex is

$$\boldsymbol{v} = \kappa \boldsymbol{b},$$

where $\boldsymbol{b}$ is the binormal to the vortex curve (see for example [12]). This is identical to the so-called local induction approximation for a classical vortex in an otherwise irrotational fluid and has been derived from the Euler equations by [5, 13] in the limit that the width of the vortex core shrinks to zero.

In two dimensions the dynamics of a curve evolving under (2) has been fairly intensively investigated. Mullins [9] found travelling waves, rotating waves and a particular class of similarity solutions. A Lie group analysis was carried out by Wood [16] which revealed the existence of other types of similarity solution which were then analysed in detail. Gage [7] showed that an embedded (non-self-intersecting) two-dimensional curve evolving under the velocity law (2) will tend to a circle before shrinking in finite time to a point. In fact it can be shown that a closed curve of length $l_1(t)$ shrinks according to the law

$$\frac{\mathrm{d}l_1}{\mathrm{d}t} = -\int_0^{l_1(t)} \kappa^2 \,\mathrm{d}l,$$

where we parametrize the curve in terms of arclength l. This result also holds in three dimensions and is called *the curve shortening property*. It can be proved by formulating (2) in terms of arclength. Self-intersecting planar curves have been considered by Altschuler [1]. Such curves develop singularities in their evolution and [1] defines the flow through such singularity to be given by the limiting flow of a sequence of space curves which asymptote to the planar curve. Furthermore, he demonstrates this limit to be independent of the sequence taken. In a sequel paper [2] singularity development was investigated for space curves and shown to be a planar phenomenon.

A theoretical treatment of the problem given by (2) can be found in a work by Ambrosio and Soner [4].

In two dimensions the curvature of the curve can be written in terms of the angle θ the curve makes to the x-axis, say, and its arclength l, so that

$$\kappa = |\theta_l|.$$

Using this formulation it can be shown that the area A enclosed by a (closed) curve decreases according to

$$\frac{\mathrm{d}A}{\mathrm{d}t} = -2\pi. \tag{3}$$

In three dimensions we can employ a similar formulation by introducing a second angle ϕ, so that the tangent to the curve

$$\boldsymbol{t} = (\sin\theta\cos\phi, \sin\theta\sin\phi, \cos\theta)\,.$$

Here it is found that the curvature is

$$\kappa = \left(\theta_l^2 + \sin^2\theta\phi_l^2\right)^{1/2}.$$

The generalization of (3) to three dimensions can be found using this formulation and is that, where ϕ is monotonically increasing (or decreasing) in s, the area of the projection of the curve onto the x–y plane A_{proj} changes according to

$$\frac{\mathrm{d}A_{\text{proj}}}{\mathrm{d}t} = -\int_0^{2\pi} \sin^2\theta \,\mathrm{d}\phi.$$

In the remainder of this work we investigate the velocity law (2) as applied to a space curve (we make no assumptions about whether the curve is self-intersecting or otherwise). We find it helpful to represent the curve by the vector $\boldsymbol{q}$ such that its position at time t is given by

$$\boldsymbol{x} = \boldsymbol{q}(s,t) = (u(s,t), v(s,t), w(s,t)),$$

in Cartesian (x, y, z) space, where s is some, as yet undefined, parametrization. The velocity law (2) can then be written in the form

$$\boldsymbol{q}_t = \kappa \boldsymbol{n} - G\boldsymbol{t}, \tag{4}$$

where the subscript denotes the partial derivative and we allow an arbitrary component of $\boldsymbol{q}_t$, magnitude G, in the tangential direction. The choice of G has the effect of determining the evolution of the parametrisation s.

In terms of the parametrisation s the tangent, the normal and the curvature of the curve are given by

$$\boldsymbol{t} = \frac{\boldsymbol{q}_s}{|\boldsymbol{q}_s|},$$
$$\kappa\boldsymbol{n} = \frac{1}{|\boldsymbol{q}_s|}\frac{\partial}{\partial s}\left(\frac{\boldsymbol{q}_s}{|\boldsymbol{q}_s|}\right), \qquad |\boldsymbol{n}| = 1.$$

It follows that the velocity law (2) can be formulated in the form

$$u_t - \frac{1}{\sqrt{u_s^2+v_s^2+w_s^2}}\left(\frac{u_s}{\sqrt{u_s^2+v_s^2+w_s^2}}\right)_s + \frac{Gu_s}{\sqrt{u_s^2+v_s^2+w_s^2}} = 0, \tag{5}$$

$$v_t - \frac{1}{\sqrt{u_s^2+v_s^2+w_s^2}}\left(\frac{v_s}{\sqrt{u_s^2+v_s^2+w_s^2}}\right)_s + \frac{Gv_s}{\sqrt{u_s^2+v_s^2+w_s^2}} = 0, \tag{6}$$

$$w_t - \frac{1}{\sqrt{u_s^2+v_s^2+w_s^2}}\left(\frac{w_s}{\sqrt{u_s^2+v_s^2+w_s^2}}\right)_s + \frac{Gw_s}{\sqrt{u_s^2+v_s^2+w_s^2}} = 0. \tag{7}$$

Useful simplifications can be made by choosing G appropriately. For instance, by setting

$$G = \left(\frac{1}{\sqrt{u_s^2+v_s^2+w_s^2}}\right)_s,$$

we can set $s = z$. Then the evolution of the curve given by $\boldsymbol{q} = (u(z,t), v(z,t), z)$ is governed by the coupled system

$$u_t = \frac{u_{zz}}{(1+u_z^2+v_z^2)}, \tag{8}$$

$$v_t = \frac{v_{zz}}{(1+u_z^2+v_z^2)}. \tag{9}$$

In terms of this parametrization the curvature κ is given by

$$\kappa = \frac{\left[(v_z u_{zz} - u_z v_{zz})^2 + u_{zz}^2 + v_{zz}^2\right]^{1/2}}{(1 + u_z^2 + v_z^2)^{3/2}}.$$

Another useful formulation is obtained by writing

$$u = r(\theta, t)\cos\theta, \qquad v = r(\theta, t)\sin\theta, \qquad w = z(\theta, t),$$

setting $s = \theta$ and

$$G = \frac{1}{\left(r_\theta^2 + z_\theta^2 + r^2\right)^{1/2}}\left(\frac{2r_\theta}{r} - \frac{r_\theta r_{\theta\theta} + z_\theta z_{\theta\theta} + r r_\theta}{r_\theta^2 + z_\theta^2 + r^2}\right).$$

This results in a system which describes the evolution of the curve in terms of the cylindrical polar coordinates r, θ and z:

$$r r_t = \frac{r r_{\theta\theta} - r^2 - 2r_\theta^2}{r_\theta^2 + z_\theta^2 + r^2}, \tag{10}$$

$$r z_t = \frac{r z_{\theta\theta} - 2r_\theta z_\theta}{r_\theta^2 + z_\theta^2 + r^2}. \tag{11}$$

In terms of this parameterisation the curvature is

$$\kappa = \frac{\left[(z_{\theta\theta} r_\theta - z_\theta r_{\theta\theta})^2 + (r z_{\theta\theta} - r_\theta z_\theta)^2 + (r_\theta^2 - r r_{\theta\theta})^2 + (r^2 + 3r_\theta^2 - 2r r_{\theta\theta})(r^2 + r_\theta^2 + z_\theta^2)\right]^{1/2}}{(r^2 + r_\theta^2 + z_\theta^2)^{3/2}}.$$

In the next section we use the formulation (8)–(9) to derive all classical Lie symmetries of (2); these are equally applicable to all formulations of (2). In Section 3 we use these symmetries to write down the similarity reductions for the formulation (10)–(11) (which turns out to be convenient to work with). In Sections 4 and 5 we look for the corresponding similarity solutions. Note that although we work with (10)–(11) we are in fact able to find solutions which are not graphs in θ by investigating the finite θ blow-up of the similarity solutions. Finally, in Section 6, we draw our conclusions.

2. Symmetries

We apply the usual Lie group method for determining the classical symmetries of (8)-(9) (see, for example, Hydon [10]), in the first instance by determining the infinitesimal transformations of the form

$$t^* \sim t + \varepsilon T(t, u, v, z), \qquad u^* \sim u + \varepsilon U(t, u, v, z),$$
$$v^* \sim v + \varepsilon V(t, u, v, z), \qquad z^* \sim z + \varepsilon Z(t, u, v, z),$$

which leave equations (8)-(9) unchanged to order ε, where $\varepsilon \ll 1$. (The notation $A \sim B$ means that $A - B$ is much smaller than the smallest term contained in B in the limit of interest (in this case

$\varepsilon \to 0$).) Omitting the details of the derivation, we find that the symmetry group of (8)-(9) has eight parameters taking the form

$$T = 2\alpha t + t_0, \tag{12}$$

$$\begin{pmatrix} U \\ V \\ Z \end{pmatrix} = \begin{pmatrix} \alpha & d & -b \\ -d & \alpha & -c \\ b & c & \alpha \end{pmatrix} \begin{pmatrix} u \\ v \\ z \end{pmatrix} + \begin{pmatrix} u_0 \\ v_0 \\ z_0 \end{pmatrix}, \tag{13}$$

where α, t_0, b, c, d, u_0, v_0 and z_0 are all arbitrary constants. We can in the usual way use the infinitesimal versions of the groups to construct the global forms of the transformations under which equations (8)-(9) are invariant. These are given by solving the initial value problem

$$\frac{\partial t^*}{\partial \varepsilon} = T(t^*, u^*, v^*, w^*), \quad \frac{\partial u^*}{\partial \varepsilon} = U(t^*, u^*, v^*, w^*), \quad \frac{\partial v^*}{\partial \varepsilon} = V(t^*, u^*, v^*, w^*), \quad \frac{\partial z^*}{\partial \varepsilon} = Z(t^*, u^*, v^*, w^*) \tag{14}$$

with

$$t^* = t, \quad u^* = u, \quad v^* = v, \quad z^* = z \qquad \text{on } \varepsilon = 0.$$

We can simplify the solution of (14) by first making a rotation of the (u^*, v^*, z^*) coordinates about an appropriate axis to leave equation (14) in the form

$$\frac{\partial t^*}{\partial \varepsilon} = 2\alpha t^* + t_0, \tag{15}$$

$$\begin{pmatrix} \dfrac{\partial u^*}{\partial \varepsilon} \\ \dfrac{\partial v^*}{\partial \varepsilon} \\ \dfrac{\partial z^*}{\partial \varepsilon} \end{pmatrix} = \begin{pmatrix} \alpha & -M & 0 \\ M & \alpha & 0 \\ 0 & 0 & \alpha \end{pmatrix} \begin{pmatrix} u^* \\ v^* \\ z^* \end{pmatrix} + \begin{pmatrix} u_0 \\ v_0 \\ z_0 \end{pmatrix}. \tag{16}$$

We note that t_0, u_0, v_0 and z_0 represent translation invariants, α a rescaling invariant and M a rotation invariant; the parameters b, c and d in (12)–(13) relate to M and the axis about which the rotation occurs. We now integrate the system (15)–(16) with respect to ε. In the case $\alpha = 0$ and $M = 0$ we have

$$t^* = t + \varepsilon t_0, \qquad u^* = u + \varepsilon u_0, \qquad v^* = v + \varepsilon v_0, \qquad z^* = z + \varepsilon z_0, \tag{17}$$

corresponding to a translation in each variable. By rotating the axes appropriately we can, without loss of generality, set $u_0 = v_0 = 0$. In the case $\alpha = 0$, $M \neq 0$ we have (where we set $u_0 = v_0 = 0$ by translation of u and v)

$$t^* = t + \varepsilon t_0, \qquad u^* = u\cos(\varepsilon M) - v\sin(\varepsilon M),$$

$$v^* = u\sin(\varepsilon M) + v\cos(\varepsilon M), \quad z^* = z + \varepsilon z_0,$$

in terms of the polar coordinates r, θ and z,

$$t^* = t + \varepsilon t_0, \qquad r^* = r, \qquad \theta^* = \theta + \varepsilon M, \qquad z^* = z + \varepsilon z_0. \tag{18}$$

Integrating (15)–(16) with respect to ε in the case $\alpha \neq 0$ (where we set $u_0 = v_0 = z_0 = t_0 = 0$ by translation of u, v, z and t) we obtain

$$\begin{aligned} t^* &= \exp(2\alpha\varepsilon)t, \\ u^* &= \exp(\alpha\varepsilon)\,(u\cos(\varepsilon M) - v\sin(\varepsilon M))\,, \\ v^* &= \exp(\alpha\varepsilon)\,(u\sin(\varepsilon M) + v\cos(\varepsilon M))\,, \\ z^* &= \exp(\alpha\varepsilon)z. \end{aligned}$$

This corresponds to a rotation about an arbitrary axis, one rescaling and four translations, as we might expect in advance from the geometrical interpretation of the motion but probably not from the partial differential equation formulation (8)-(9). Writing this in terms of the polar coordinates r, θ and z gives

$$t^* = \exp(2\alpha\varepsilon)t, \qquad r^* = \exp(\alpha\varepsilon)r, \qquad \theta^* = \theta + M\varepsilon, \qquad z^* = \exp(\alpha\varepsilon)z. \tag{19}$$

3. Similarity reductions

The case $\alpha = 0$, $M = 0$. We now note the invariants (i.e. quantities which are not functions of ε) of the global transformation (17) when $u_0 = v_0 = 0$; they are

$$u, \quad v \quad z - qt,$$

where $q = z_0/t_0$. This leads to a travelling wave reduction to (8)-(9) of the form

$$u = U(z - qt), \qquad v = V(z - qt). \tag{20}$$

The case $\alpha = 0$, $M \neq 0$. Invariants of the global transformation (18) are

$$\theta - ct, r = \left(u^2 + v^2\right)^{1/2}, z - qt,$$

where $c = M/t_0$. These suggest that we should use the equations describing the evolution of the filament in polar coordinates, namely (10) and (11), to look for a travelling rotating wave solution to $\boldsymbol{v} = \kappa\boldsymbol{n}$ of the form

$$r = R(\theta - c\,t), \qquad z = q\,t + f(\theta - c\,t), \tag{21}$$

where the arbitrary constants q and c are, respectively, the velocity of the wave in the z-direction and its angular velocity about the z-axis. Note that the travelling wave ansatz (20) corresponds to the special case of the travelling rotating wave ansatz (21) where $c = 0$. We return to both of these reductions shortly. In the exceptional case where $t_0 = 0$ as well as $\alpha = 0$ the invariants of the transformation are

$$z - k\theta, \qquad t, \qquad r,$$

where $k = z_0/M$ and we therefore look for a similarity reduction to equations (10) and (11) of the form

$$z = k\,\theta + f(t), \qquad r = R(t), \tag{22}$$

where k is some constant. This gives rise to a contracting helix (see for example [2, 6]) such that when we substitute (22) into (10) and (11) we find that f is a constant (which may, without any loss of generality, be taken to be zero) and $R(t)$ is given by

$$t = \frac{1}{2}(R_0^2 - R^2) + k^2 \log\left(\frac{R_0}{R}\right),$$

where $R(0) = R_0$. Hence as $t \to \infty$ the radius decreases as $\exp(-t/k^2)$.

The case $\alpha \neq 0$. Invariants of the global transformation (19) are

$$\frac{r^2}{t} = \frac{u^2 + v^2}{t}, \qquad \frac{z^2}{t}, \qquad \theta - \frac{M}{2\alpha}\log|t|.$$

We thus look for similarity reductions to (10)-(11) either of the form

$$r = \sqrt{t}\, R(\theta - p\log t), z = \sqrt{t}\, f(\theta - p\log t), \tag{23}$$

or of the form

$$r = \sqrt{-t}\, R(\theta + p\log(-t)), w = \sqrt{-t}\, f(\theta + p\log(-t)), \tag{24}$$

where p is an arbitrary constant.

We now have a complete catalogue of the classical similarity reductions to the system of partial differential equations (8) and (9) describing motion by curvature of a curve parametrised by z and t and equivalently to the system of partial differential equations (10) and (11) describing motion by curvature of a curve parametrised by θ and t.

4. Rotating travelling waves

4.1 *Formulation*

In light of (21), we look for a solution to (10)–(11) of the form

$$r = R(\eta), \qquad z = qt + f(\eta), \qquad \eta = \theta - ct.$$

This ansatz results in the following system of ordinary differential equations:

$$R'' + cR'\left(R^2 + f'^2 + R'^2\right) - \left(R + \frac{2R'^2}{R}\right) = 0, \tag{25}$$

$$f'' + \left(cf' - q\right)\left(R^2 + f'^2 + R'^2\right) - \frac{2R'f'}{R} = 0, \tag{26}$$

which is a third-order autonomous system for R and f'; the only symmetries of the original partial differential equations inherited by this coupled system are invariance under translations in f and η. It is, however, invariant under the discrete transformation

$$\eta \to -\eta, \qquad c \to -c$$

and we therefore choose, without any loss of generality, $c > 0$ in all that follows. It should also be noted that, for non-zero c, we can reduce the number of free parameters in the problem to one, namely $q/\sqrt{c}$, by rescaling f and R with $1/\sqrt{c}$. We first describe the possible asymptotic forms of solutions to (25)–(26) and then outline how they can be used to formulate initial value problems which furnish meaningful solutions to (10)–(11).

4.2 *Finite η blow-up*

The balance

$$R'' \sim -cR'\left(f'^2 + R'^2\right), \qquad f'' \sim -cf'\left(f'^2 + R'^2\right),$$

in (25) and (26) arises in describing blow-up at finite η (in this case to R' and f' becoming unbounded). The corresponding asymptotic expressions for R and f are thus

$$R \sim d + \left(\frac{2(\eta-\eta_0)}{c}\right)^{1/2}\cos\alpha, \qquad f \sim h + \left(\frac{2(\eta-\eta_0)}{c}\right)^{1/2}\sin\alpha, \tag{27}$$

or

$$R \sim d - \left(\frac{2(\eta-\eta_0)}{c}\right)^{1/2}\cos\alpha, \qquad f \sim h - \left(\frac{2(\eta-\eta_0)}{c}\right)^{1/2}\sin\alpha, \tag{28}$$

where α, d, h and η_0 are all arbitrary constants. It is clear that there are four degrees of freedom for this asymptotic behaviour (since it contains four arbitrary constants), the maximum possible for the fourth-order system (25) and (26), so this is a generic form of blow-up. There is also a second type of blow-up which can occur as $R \to 0$. Here there is a local balance of the form

$$R'' + cR'\left(f'^2 + R'^2\right) \sim \frac{2R'^2}{R}, \qquad f'' + cf'\left(f'^2 + R'^2\right) \sim \frac{2R'f'}{R},$$

with the corresponding asymptotic behaviour

$$R \sim \left(\frac{6(\eta-\eta_0)}{c}\right)^{1/2}\cos\alpha, \qquad f \sim h + \left(\frac{6(\eta-\eta_0)}{c}\right)^{1/2}\sin\alpha, \tag{29}$$

or

$$R \sim -\left(\frac{6(\eta-\eta_0)}{c}\right)^{1/2}\cos\alpha, \qquad f \sim h - \left(\frac{6(\eta-\eta_0)}{c}\right)^{1/2}\sin\alpha. \tag{30}$$

In this case it is not obvious how many degrees of freedom are contained in this asymptotic behaviour; to assess this we perturb about (29) (an equivalent analysis applies to (30)) by substituting

$$R \sim \left(\frac{6(\eta-\eta_0)}{c}\right)^{1/2}\cos\alpha + R_1, \qquad f \sim h + \left(\frac{6(\eta-\eta_0)}{c}\right)^{1/2}\sin\alpha + f_1,$$

into equations (25)–(26), linearizing in R_1 and f_1 and seeking the eigenmodes (and therefore neglecting the forcing terms) to obtain a fourth-order homogeneous system. The solution of this linear system (at leading order in $(\eta-\eta_0)$) reveals the eigenmodes

$$\left.\begin{aligned} R_1 &= 0 \\ f_1 &= 1 \end{aligned}\right\}; \qquad \left.\begin{aligned} R_1 &\sim \cot\alpha(\eta-\eta_0)^{-1/2} \\ f_1 &\sim (\eta-\eta_0)^{-1/2} \end{aligned}\right\};$$
$$\left.\begin{aligned} R_1 &\sim -\tan\alpha(\eta-\eta_0)^{1/2} \\ f_1 &\sim (\eta-\eta_0)^{1/2} \end{aligned}\right\}; \qquad \left.\begin{aligned} R_1 &\sim \cot\alpha(\eta-\eta_0)^{-1} \\ f_1 &\sim (\eta-\eta_0)^{-1} \end{aligned}\right\}. \tag{31}$$

The first of these corresponds to a small change in h, the second to a small change in η_0 and the third to a small change in α; the fourth is larger than (29) and is hence asymptotically inconsistent, from which we conclude that (29) and (30) have three degrees of freedom. This is as might be expected since the degree of freedom d in (27)–(28) is lost by requiring blow-up to occur as $R \to 0$.

We believe these to be the only types of finite η blow-up which can occur for (25)–(26). Note that for $c > 0$ blow-up can only occur as η tends to η_0 from above and for $c < 0$ only as η tends to η_0 from below. Hence only one blow-up can occur along any given solution.

4.3 *Behaviour of the solution for large η*

As $\eta \to +\infty$ we find the following balance between terms in equations (25)–(26):

$$cR^2R' \sim R, \qquad cR^2f' \sim qR^2,$$

with asymptotic behaviour

$$R \sim \left(\frac{2\eta}{c}\right)^{1/2}, \qquad f \sim \frac{q\eta}{c}. \tag{32}$$

We now again determine the number of degrees of freedom exhibited by this asymptotic behaviour. Writing

$$R \sim \left(\frac{2\eta}{c}\right)^{1/2} + R_1, \tag{33}$$

$$f \sim \frac{q\eta}{c} + f_1, \tag{34}$$

substituting into (25)–(26), linearizing in R_1 and f_1 and neglecting forcing terms gives a homogeneous system for R_1 and f_1 which has the following possible asymptotic behaviours for large η:

$$\left.\begin{aligned} R_1 &= 0 \\ f_1 &= 1 \end{aligned}\right\}; \qquad \left.\begin{aligned} R_1 &\sim \eta^{-1/2} \\ f_1 &\sim \frac{q}{2\,(2c)^{1/2}}\eta^{-2} \end{aligned}\right\};$$

$$\left.\begin{aligned} R_1 &\sim -\frac{\exp(-\eta^2)}{2\eta} \\ f_1 &\sim -q\left(\frac{2}{c}\right)^{1/2}\eta^{-1/2}\exp(-\eta^2) \end{aligned}\right\}; \qquad \left.\begin{aligned} R_1 &\sim q\left(\frac{2}{c}\right)^{1/2}\eta^{-1/2}\exp(-\eta^2) \\ f_1 &\sim -\frac{\exp(-\eta^2)}{2\eta} \end{aligned}\right\}.$$

None of these expressions leads to a violation of the asymptotic expansions (33)–(34), so there are four degrees of freedom exhibited by the behaviour (32) which is therefore generic.

We also consider the asymptotic behaviour of solutions which do not exhibit finite η blow-up in the limit as $\eta \to -\infty$, by making the ansatz

$$R \sim k\exp(\alpha\eta), \qquad f \sim d\eta, \qquad \alpha > 0. \tag{35}$$

Substitution into (25)–(26) gives two relations for α and d:

$$cd^3 - qd^2 - 2\alpha d = 0, \qquad \alpha^2 - c\,d^2\alpha + 1 = 0,$$

so that

$$d = \pm\left(\frac{q^2}{2c^2} + \left(\frac{q^4}{4c^4} + \frac{4}{c^2}\right)^{1/2}\right)^{1/2}, \qquad \alpha = \frac{1}{2}d(c\,d - q), \tag{36}$$

and k is an arbitrary constant. Again, we can determine the number of degrees of freedom exhibited in this behaviour by linearizing about (35):

$$R \sim k\exp(\alpha\eta) + R_1, \qquad f \sim d\eta + f_1,$$

implying that R_1 and f_1 are made up of linear combinations of the following expressions:

$$\left.\begin{matrix} R_1 = 0 \\ f_1 = 1 \end{matrix}\right\};\quad \left.\begin{matrix} R_1 \sim \exp(\alpha\eta) \\ \log f_1 \sim 2\alpha\eta \end{matrix}\right\};\quad \left.\begin{matrix} R_1 \sim \exp((\alpha - cd^2)\eta)\left(\dfrac{k\alpha}{d}\sin(d\mu\eta) + \dfrac{k\mu}{2}\cos(d\mu\eta)\right) \\ f_1 \sim \exp(-cd^2\eta)\sin(d\mu\eta) \end{matrix}\right\};$$

$$\left.\begin{matrix} R_1 \sim \exp((\alpha - cd^2)\eta)\left(\dfrac{k\alpha}{d}\cos(d\mu\eta) - \dfrac{k\mu}{2}\sin(d\mu\eta)\right) \\ f_1 \sim \exp(-cd^2\eta)\cos(d\mu\eta) \end{matrix}\right\}.$$

Here $\mu^2 = \sqrt{q^4/4 + 4c^2} - q^2/2$. The first and second of these behaviours represent a change in f by a small constant and a small change in k. However, since we look at the behaviour as $\eta \to -\infty$ and have assumed $c > 0$ we require that the third and fourth of these be absent in order that the asymptotics are not violated. It follows that there are only two degrees of freedom represented in the behaviour (35).

4.4 *Construction of rotating travelling wave solutions to* $\boldsymbol{v} = \kappa\boldsymbol{n}$

Three distinct types of solution to $\boldsymbol{v} = \kappa\boldsymbol{n}$ may be formed using solutions to (25)–(26) with different asymptotic behaviours. Examples of these three sorts of solution are given in Figs 1 and 2, in which the solution is represented by a curve, fattened for visibility, plotted as a function of $R(\eta)\cos(\eta)$, $R(\eta)\sin(\eta)$ and $f(\eta)$ (in other words, showing the curve as it appears in Cartesian coordinates (x, y, z) at time $t = 0$). Outlined below are the three possible ways in which it is possible to form a smooth rotating travelling wave solution.

(1.) We can join a solution with asymptotic behaviour (29) as $\eta \to \eta_0^+$ to one with asymptotic behaviour (30) as $\eta \to \eta_0^+$ to find a regular solution of $\boldsymbol{v} = \kappa\boldsymbol{n}$ in which R and f are multivalued. Both branches exhibit the asymptotic behaviour (32) as $\eta \to +\infty$ (which has four degrees of freedom). In practice this construction involves choosing η_0, h and α shooting from η slightly larger than η_0 towards $\eta = \infty$ along one branch (using (29)) and then repeating the process along the other branch. An example (with $\eta_0 = 0$, $h = 0$ and $\alpha = \pi/4$) of such a solution is given in Fig. 1(a). The curve shown in this figure rotates in an anti clockwise direction about the z (i.e. the f) axis while translating in the positive z direction. An animation of the motion of this curve can be found in [15].

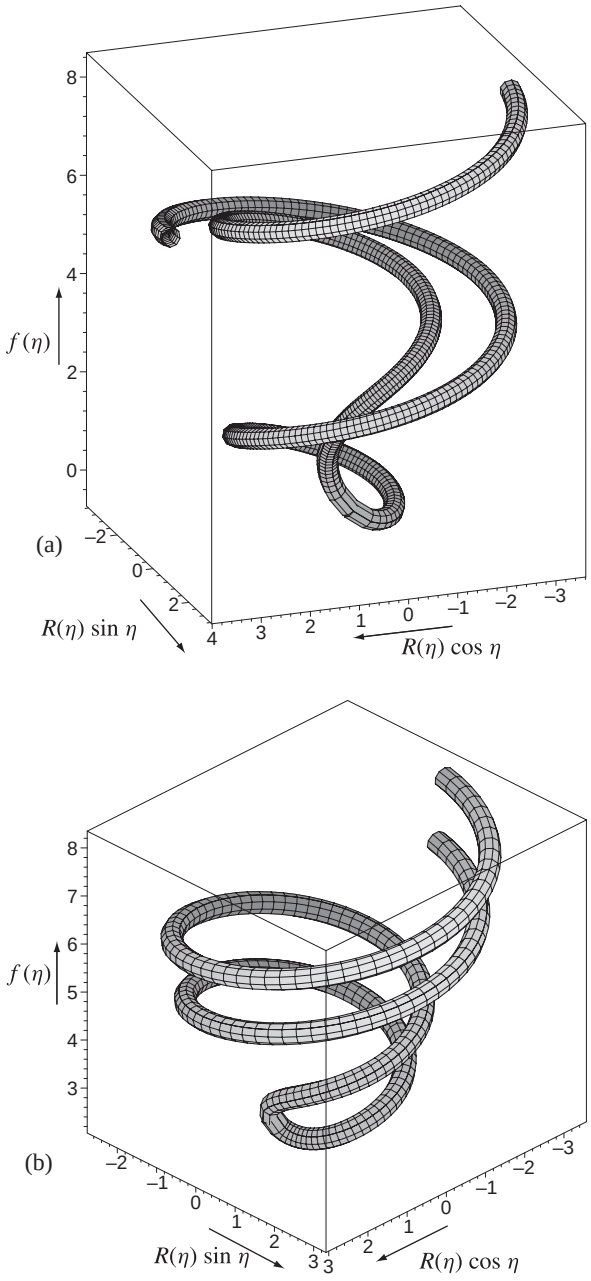

FIG. 1. Examples of rotating travelling waves. (a) A solution with $c = 1.5$ and $q = 1.0$ with initial conditions $R \sim \pm\cos(\pi/4)\sqrt{4\eta}$ and $f \sim \pm\sin(\pi/4)\sqrt{4\eta}$ as $\eta \to 0$. (b) A solution with $c = 2.0$ and $q = 1.0$ with initial conditions $R \sim \cos(3\pi/8)(3 \pm \sqrt{\eta})$ and $f \sim \sin(3\pi/8)(3 \pm \sqrt{\eta})$ as $\eta \to 0$.

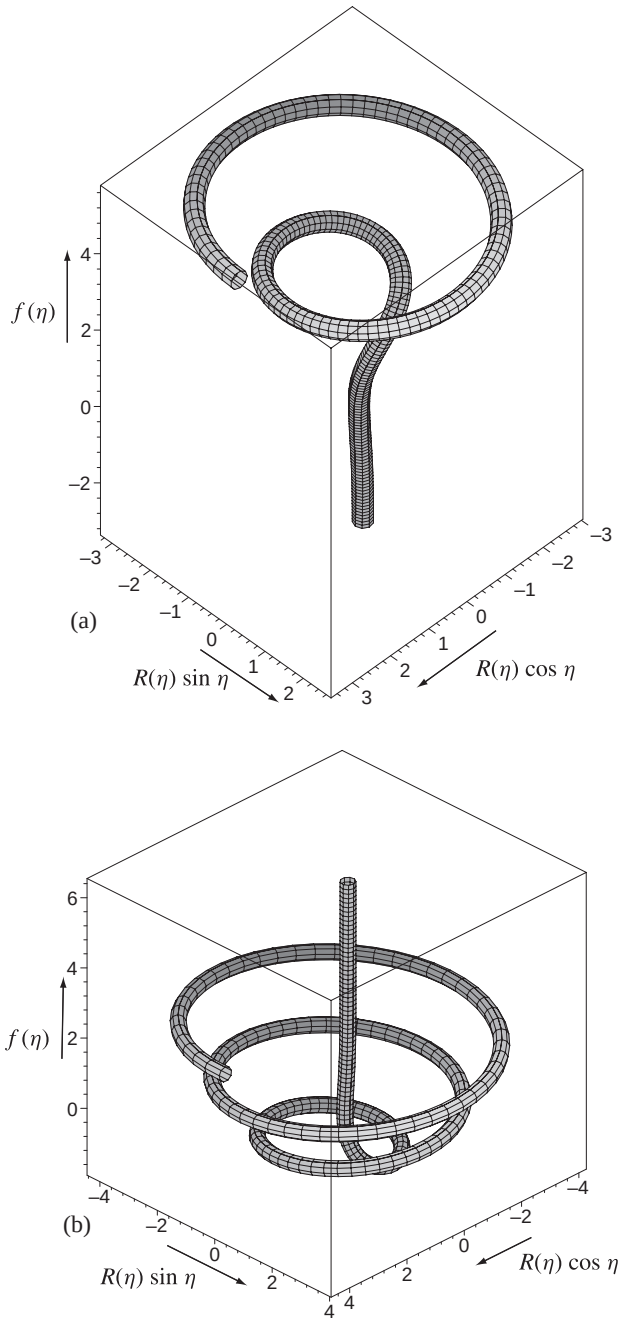

FIG. 2. Examples of a further kind of travelling rotating wave with $c = 2.0$ and $q = 0.5$ and initial data compatible with the asymptotic behaviour given by (35) as $\eta \to -\infty$. In (a) the positive root of d is taken and in (b) the negative.

(2.) We can also join a solution with asymptotic behaviour (27) as $\eta \to \eta_0^+$ to one with asymptotic behaviour (28) as $\eta \to \eta_0^+$. The resulting curve is a regular solution of $\boldsymbol{v} = \kappa \boldsymbol{n}$ but is again multivalued in R and f. The two branches both exhibit the asymptotic behaviour (32) as $\eta \to +\infty$, which has four degrees of freedom. The practical details of the computation are the same as above. An example of such a solution is given in Fig. 1(b) (with $\eta_0 = 0$, $h = 3\sin(3\pi/8)$, $d = 3\cos(3\pi/8)$, and $\alpha = (3\pi/8)$). The curve shown in this figure again rotates in an anti clockwise direction about the z (i.e. the f) axis while translating in the positive z direction.

(3.) We can find solutions with asymptotic behaviour (35) as $\eta \to -\infty$ and asymptotic behaviour (32) as $\eta \to +\infty$. This involves using (35) in shooting from $\eta = -\infty$, where there are two degrees of freedom, to $\eta = \infty$ where there are four degrees of freedom. Examples of such solutions are given in Figs 2(a) and (b). In both cases $k = 0.1$, $c = 2.0$ and $q = 0.5$ and α and d are calculated using (36). However, in the former the positive root of d is taken while in the latter the negative root is taken. The curve shown in Fig. 2(a) rotates in an anti clockwise direction about the z (i.e. the f) axis and propagates in the positive z direction leaving a straight line in its wake. The curve in Fig. 2(b) rotates and translates in a similar fashion. However, as it does so it consumes the half-line lying along the z-axis.

Solutions to the ODEs (25)–(26) were calculated numerically using a fourth-order Runge–Kutta method. In cases 1 and 2 we used the appropriate asymptotic behaviours about $\eta = \eta_0$ to construct the initial values for the solution at an initial point $\eta = \eta_0 + \delta$ where $0 < \delta \ll 1$. In case 3 we used (35) to construct initial values for the solution at $\eta = -1/\delta$, where again $0 < \delta \ll 1$. Solutions of type 1 are characterized by three arbitrary parameters α, h and η_0 (since three degrees of freedom are exhibited by the initial conditions (29) and (30)); the last of these parameters η_0 corresponds to a translation of the curve along the f-axis. Such solutions pass through the axis of rotation. Solutions of type 2 are characterized by four parameters α, d, h and η_0 (since four degrees of freedom are exhibited by the initial conditions (27) and (28)); again η_0 corresponds to a translation of the curve along the f-axis. Solutions of type 3 are characterized by two arbitrary parameters (since two degrees of freedom are exhibited by (35)). In all cases considered the numerical behaviour for large positive η was compatible with (32) which should not be surprising as it has four degrees of freedom.

4.5 *Special cases*

4.5.1 $q = 0$*: rotating waves.* When $q = 0$ in equations (25)–(26) the equations describe a rotating wave with angular velocity c. While these have the same asymptotic behaviour as before close to blow up (i.e. (27)–(28) and (29)–(30)), they exhibit different behaviour as $\eta \to +\infty$ where the balance is of the form

$$cR'R^2 - R \sim 0, \qquad f'' + cf'R^2 \sim 0,$$

with asymptotic behaviour

$$R \sim \left(\frac{2\eta}{c}\right)^{1/2}, \qquad f \sim d, \tag{37}$$

where d is an arbitrary constant. Hence as $\eta \to +\infty$ the solution tends towards a planar solution. We determine the number of degrees of freedom exhibited by this behaviour by linearizing about

(37) in the form

$$R \sim \left(\frac{2\eta}{c}\right)^{1/2} + R_1, \qquad f \sim d + f_1,$$

and find that R_1 and f_1 are composed of linear combinations of

$$\left.\begin{matrix} R_1 = 0 \\ f_1 \sim 1 \end{matrix}\right\}; \quad \left.\begin{matrix} R_1 \sim \eta^{-1/2} \\ f_1 = 0 \end{matrix}\right\}; \quad \left.\begin{matrix} R_1 \sim \dfrac{1}{2\eta}\exp(-\eta^2) \\ f_1 = 0 \end{matrix}\right\}; \quad \left.\begin{matrix} R_1 = 0 \\ f_1 \sim \dfrac{1}{2\eta}\exp(-\eta^2) \end{matrix}\right\}.$$

Since none of these behaviours violates the asymptotic expansion (37) in the limit $\eta \to +\infty$ four degrees of freedom are exhibited by (37).

Rotating waves can be constructed in an identical manner to rotating travelling waves. Examples of rotating waves computed from equations (25)–(26) are plotted in Figs 3 and 4. In Fig. 3(a) the curve is formed from two solutions with initial data given by (27) and (28) whilst in Fig. 3(b) it is formed from two solutions with asymptotic behaviours (29) and (30). Figure 4 shows a rotating wave which has asymptotic behaviour of the form (35) as $\eta \to -\infty$. In all three cases the curve rotates in an anti clockwise fashion about the f-axis. Figure 4 is of particular interest because it suggests that, when the forcing term $(\nabla \wedge \boldsymbol{B}) \wedge \boldsymbol{t}$ is retained in the superconducting vortex equation of motion (1), that it is possible to form a three-dimensional superconducting analogue of the Frank–Read source seen in disclination dynamics. In this scenario a superconducting vortex is pinned on two semi-infinite lines and curves round from the top of one line to meet the top of the other. When a current (i.e. an external force) is applied to this structure it seems likely that it would generate a lengthening double-spiral vortex that would, after sufficient time, reconnect with itself releasing a vortex ring.

4.5.2 $c = 0$*: travelling waves.* When $c = 0$, equations (25)–(26) describe a travelling wave moving with velocity q in the z-direction. In particular, we can now identify the similarity variable as θ and write equation (25) in the form

$$\frac{\mathrm{d}^2 R}{\mathrm{d}\theta^2} - \left(R + \frac{2}{R}\left(\frac{\mathrm{d}R}{\mathrm{d}\theta}\right)^2\right) = 0. \tag{38}$$

This has general solution

$$R = \frac{k}{\sin(\theta - \theta_0)},$$

where k and θ_0 are arbitrary constants. It follows that the solution curve lies in the plane $y\cos(\theta_0) - x\sin(\theta_0) = k$ and, as such, is equivalent to the planar solutions studied previously by Mullins [9] and Wood [16].

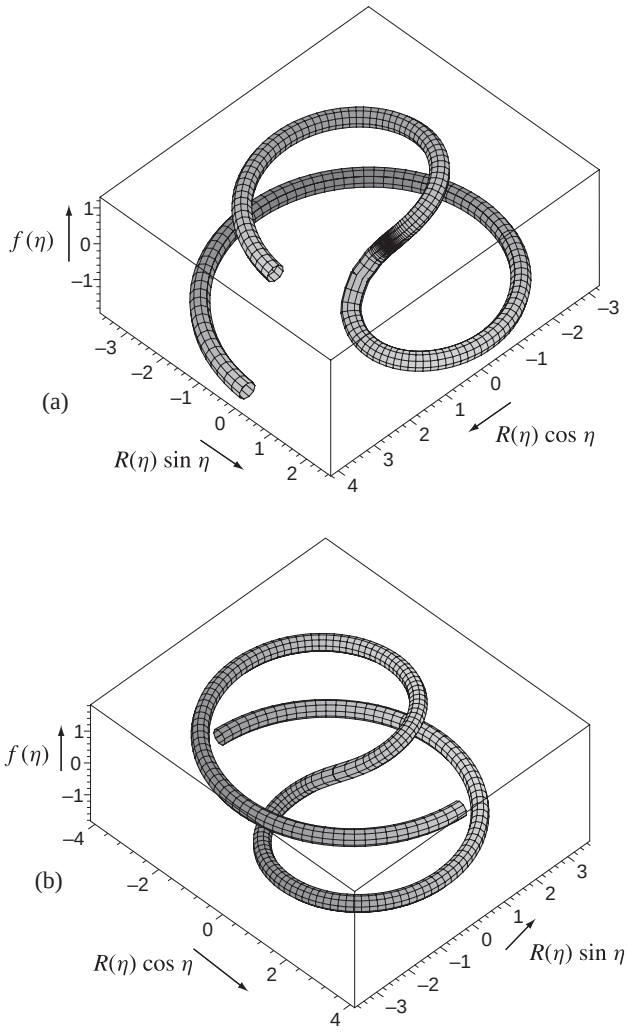

FIG. 3. (a) An example of an asymmetric rotating wave with initial conditions $R \sim \cos(-\pi/4)(1 \pm \sqrt{2\eta})$ and $f \sim \sin(-\pi/4)(1 \pm \sqrt{2\eta})$ as $\eta \to 0$. (b) An antisymmetric rotating wave with initial conditions $R \sim \pm\cos(\pi/4)\sqrt{6\eta}$ and $f \sim \pm\sin(\pi/4)\sqrt{6\eta}$ as $\eta \to 0$. In both cases $c = 1$.

5. Logarithmic similarity reductions

5.1 *Expanding case*

We now investigate similarity solutions to equations (10) and (11) of the form

$$r = \sqrt{t}\,R(\eta),$$
$$z = \sqrt{t}\,f(\eta),$$
$$\eta = \theta - p\log(t).$$

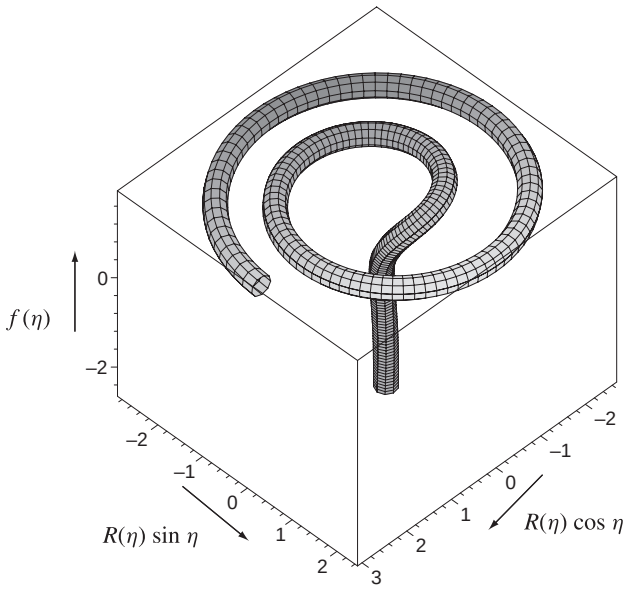

FIG. 4. An example of a further kind of rotating wave with $c = 3.0$ and initial data compatible with the asymptotic behaviour $f \sim d\eta$, $R \sim 0.1\exp(\alpha\eta)$ as $\eta \to +\infty$.

Substituting this into (10) and (11) yields the autonomous system

$$R'' = \frac{1}{2}\left(R - 2pR'\right)\left(R^2 + f'^2 + R'^2\right) + \left(R + \frac{2R'^2}{R}\right), \tag{39}$$

$$f'' = \frac{1}{2}\left(f - 2pf'\right)\left(R^2 + f'^2 + R'^2\right) + \frac{2R'f'}{R}. \tag{40}$$

Since these equations are invariant under the transformation

$$\eta \to -\eta, \qquad p \to -p,$$

we can, without loss of generality, choose $p > 0$. As with the rotating travelling wave we find two types of blow-up in finite η, namely

$$R \sim d \pm \left(\frac{2(\eta - \eta_0)}{p}\right)^{1/2} \cos\alpha, \qquad f \sim h \pm \left(\frac{2(\eta - \eta_0)}{p}\right)^{1/2} \sin\alpha, \tag{41}$$

and

$$R \sim \pm\left(\frac{6(\eta - \eta_0)}{p}\right)^{1/2} \cos\alpha, \qquad f \sim h \pm \left(\frac{6(\eta - \eta_0)}{p}\right)^{1/2} \sin\alpha, \tag{42}$$

where d, h, η_0 and α are all arbitrary constants. It follows that there are four degrees of freedom for the asymptotic behaviour (41). In order to determine the number of degrees of freedom exhibited

by the asymptotic behaviour (42) we follow the procedure adopted in the case of the equivalent behaviour of the rotating travelling wave. The result is identical to that found in (31) if we replace c by p and, as in the case of equation (29), the asymptotic behaviour (42) has three degrees of freedom.

The large η behaviour differs from the previous case. Equations (39) and (40) have no finite stationary points and hence for η increasing the only possible asymptotic behaviour is for at least one of f and R to tend to infinity. Hence we find that

$$f \sim 2pf', \qquad R \sim 2pR',$$

so that the asymptotic behaviour is given by

$$R \sim e_1 \exp\left(\frac{\eta}{2p}\right), \qquad f \sim e_2 \exp\left(\frac{\eta}{2p}\right), \qquad \text{as } \eta \to +\infty, \tag{43}$$

where e_1 is a non-zero, but otherwise arbitrary, constant and e_2 is an arbitrary constant. If we linearise in R_1 and f_1 via the ansatz

$$R \sim e_1 \exp\left(\frac{\eta}{2p}\right) + R_1,$$
$$f \sim e_2 \exp\left(\frac{\eta}{2p}\right) + f_1,$$

we find that the asymptotic behaviour for R_1 and f_1 is a linear combination of

$$\left.\begin{aligned} R_1 &\sim \exp\left(\frac{\eta}{2p}\right) + O\left(-\exp\left(\frac{\eta}{2p}\right)\right) \\ f_1 &= O\left(\exp\left(-\frac{3\eta}{2p}\right)\right) \end{aligned}\right\}; \qquad \left.\begin{aligned} R_1 &= O\left(\exp\left(-\frac{\eta}{2p}\right)\right) \\ f_1 &\sim \exp\left(\frac{\eta}{2p}\right) \end{aligned}\right\}.$$

and two very rapidly decaying solutions each of which satisfies

$$\log R_1 \sim -p^2E^2 \exp\left(\frac{\eta}{p}\right) \qquad \log f_1 \sim -p^2E^2 \exp\left(\frac{\eta}{p}\right),$$

as $\eta \to +\infty$, where $E^2 = e_1^2 + (e_1^2 + e_2^2)/(4p^2)$. An appropriate combination of the first two of these solutions represents translational invariance (in η) of (39) and (40). Corrections to the last two solutions can be determined by proceeding to next order in the expansion (43). None of the expressions we have found for R_1 and f_1 violate the asymptotic behaviour (43); it hence exhibits four degrees of freedom.

Looking at the asymptotic behaviour (43) it might be conjectured that (by choosing $e_1 = 0$ and $e_2 \neq 0$) it is possible to find solutions to (39) and (40) which asymptote to the f-axis as $\eta \to +\infty$. However, if $f \sim e_2 \exp(\eta/(2p))$ as $\eta \to +\infty$ and $R \ll f$ then R obeys the approximate equation

$$R'' \sim \frac{e_2^2}{8p^2} \exp\left(\frac{\eta}{p}\right)\left(R - 2pR'\right) + \left(R + \frac{2R'^2}{R}\right).$$

In this limit the above equation has possible asymptotic behaviours

$$R \sim \exp\left(\frac{\eta}{2p}\right) C_1 \exp\left(\frac{e_2^2}{4} \exp\left(\frac{\eta}{p}\right)\right), \qquad R \sim C_2 \exp\left(\frac{\eta}{2p}\right),$$

where C_1 and C_2 are arbitrary constants. This suggests that the only solutions to (39) and (40) which asymptote to the f-axis as $\eta \to \infty$ are those for which $R \equiv 0$ (i.e. lie along the f-axis).

We conjecture that there is no solution to (39)–(40) which does not exhibit finite η blow up for sufficiently large negative η.

Numerical solutions. In a manner similar to that outlined above, we may join two solutions with asymptotic behaviours (41) (but different signs) to each other. We calculate the two branches separately using the positive sign in (41) to give initial conditions at $\eta = \eta_0^+$ of one branch and the negative sign in (41) to give initial conditions at $\eta = \eta_0^+$ for the other branch. For both branches we then integrate forward in η using a fourth-order Runge–Kutta numerical scheme. The behaviour as $\eta \to +\infty$ is then found to be given by (43). A typical curve obtained using this procedure is plotted in Fig. 5(b). In a similar fashion we can use the positive sign in the asymptotic behaviour (42) to provide initial conditions to calculate one branch of a continuous curve and the negative sign in equation (42) to calculate the other branch and, as before, the behaviour as $\eta \to +\infty$ is given by (43). An example of such a curve is plotted in Fig. 5(a). In both cases the curve rotates in an anti clockwise direction about the f-axis with slowing angular velocity; it expands as it does so. An animation of the curve in Fig. 5(b) can be found in [15].

The initial value problem. We may interpret solutions to (39)–(40) as satisfying an initial value problem for the original partial differential equations (10)–(11). For any fixed value of θ the corresponding value of η as $t \to 0$ tends to $+\infty$ if $p > 0$. Initial data at $t = 0$ is thus given by the large η behaviour (43). On substituting this into the similarity ansatz (23) we see that the initial data is given by two logarithmic spirals, joined at $r = 0\, z = 0$ and distorted in the z-direction to lie on the surface of a cone, that is

$$r = e_1^+ \exp\left(\frac{\theta}{2p}\right),\ z = e_2^+ \exp\left(\frac{\theta}{2p}\right),\ \text{at } t = 0,$$

and

$$r = e_1^- \exp\left(\frac{\theta}{2p}\right),\ z = e_2^- \exp\left(\frac{\theta}{2p}\right),\ \text{at } t = 0.$$

This initial value problem gives a dramatic demonstration of the curve shortening property, since the spiral is initially of infinite length in the neighbourhood of the origin but instantaneously shortens to a finite length there.

5.2 *Contracting case*

We look for solutions to (10) and (11) of the form

$$r = \sqrt{-t}\,R(\eta),\ w = \sqrt{-t}\,f(\eta),\ \eta = \theta + p\log(-t),$$

yielding

$$R'' + \frac{1}{2}\left(R + 2pR'\right)\left(R^2 + f'^2 + R'^2\right) - \left(R + \frac{2R'^2}{R}\right) = 0, \tag{44}$$

$$f'' + \frac{1}{2}\left(f + 2pf'\right)\left(R^2 + f'^2 + R'^2\right) - \frac{2R'f'}{R} = 0. \tag{45}$$

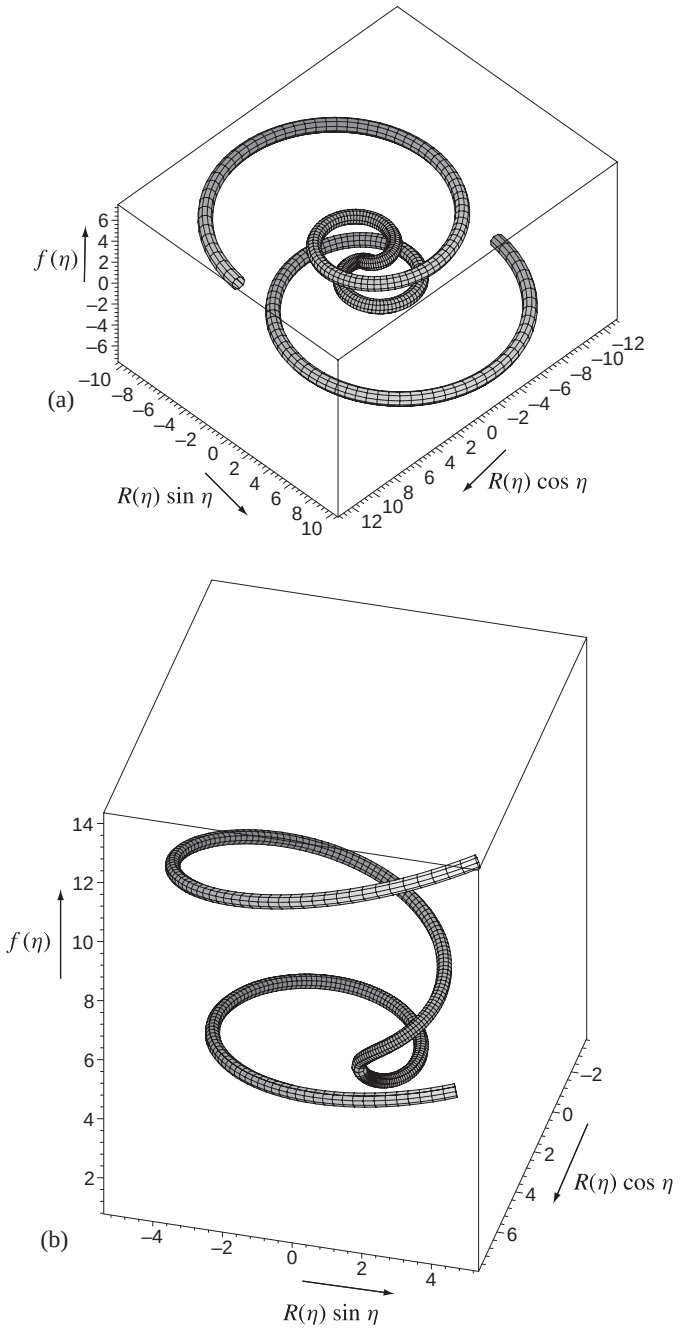

FIG. 5. (a) An example of an expanding logarithmic similarity solution with $p = 3$ and initial conditions $R \sim \pm\cos(\pi/4)\sqrt{2\eta}$ and $f \sim \pm\sin(\pi/4)\sqrt{2\eta}$ as $\eta \to 0$. (b) An asymmetric expanding logarithmic similarity solution with $p = 2$ and initial conditions $R \sim \cos(3\pi/8)(2 \pm \sqrt{\eta})$ and $f \sim \sin(3\pi/8)(2 \pm \sqrt{\eta})$ as $\eta \to 0$.

As with the expanding case these equations are invariant under

$$\eta \to -\eta, \qquad p \to -p,$$

and this allows us to choose, without any loss of generality, $p > 0$. With this choice of sign for p we find the system (44)–(45) exhibits identical finite η blow-up to equations (39)–(40), namely that given by (41) and (42), and these again have four and three degrees of freedom, respectively.

Unlike equations (39)–(40) for the expanding case, equations (44)–(45) have a critical point at $R = \sqrt{2}$, $f = 0$. Furthermore, this critical point is stable for $p > 0$. We conjecture that all solutions (with $p > 0$) tend towards this point as $\eta \to +\infty$.

As $\eta \to -\infty$ those solutions which do not exhibit finite η blow-up have asymptotic behaviour

$$R \sim e_1 \exp\left(-\frac{\eta}{2p}\right), \qquad f \sim e_2 \exp\left(-\frac{\eta}{2p}\right). \tag{46}$$

We investigate the number of degrees of freedom exhibited in this behaviour by making a perturbation to it of the form

$$R \sim e_1 \exp\left(-\frac{\eta}{2p}\right) + R_1, \tag{47}$$

$$f \sim e_2 \exp\left(-\frac{\eta}{2p}\right) + f_1, \tag{48}$$

and linearizing in R_1 and f_1. We find that the asymptotic behaviour of R_1 and f_1 is given by a linear combination of

$$\left.\begin{aligned} R_1 &= \exp\left(-\frac{\eta}{2p}\right) + O\left(\exp\left(\frac{\eta}{2p}\right)\right) \\ f_1 &= O\left(\exp\left(\frac{3\eta}{2p}\right)\right) \end{aligned}\right\}, \qquad \left.\begin{aligned} R_1 &= O\left(\exp\left(\frac{\eta}{2p}\right)\right) \\ f_1 &\sim \exp\left(\frac{-\eta}{2p}\right) \end{aligned}\right\},$$

and two rapidly decaying solutions whose leading-order behaviour is given by

$$\log R_1 \sim -p^2E^2 \exp\left(-\frac{\eta}{p}\right) \qquad \log f_1 \sim -p^2E^2 \exp\left(-\frac{\eta}{p}\right),$$

where $E^2 = e_1^2 + (e_1^2 + e_2^2)/(4p^2)$. Corrections to the leading-order behaviour of these two solutions can be determined by proceeding to the next order in the expansion (46). Since we consider the limit $\eta \to -\infty$ and $p > 0$ the first and second solutions we found for R_1 and f_1 violate the asymptotics while the third and fourth do not. Hence there are only two degrees of freedom for the asymptotic behaviour (47) and (48).

Numerical solutions. Again, as for the expanding case, we may join two solutions with initial conditions given by the asymptotic behaviours (41) (but different signs) to each other to construct a contracting logarithmic similarity solution; and we may also join two solutions with initial conditions given by asymptotic behaviours (42) (but different signs) to form a different type of contracting logarithmic similarity solution. In both cases, as $\eta \to +\infty$, the curve asymptotes to

the critical point $R = \sqrt{2},\ f = 0$ making infinitely many rotations as it does so but never self-intersecting. Examples of a curve with initial conditions of the form (41) and (42) are given in Figs 6(a) and (b) respectively. In Fig. 6(a) we have $\eta_0 = 0$, $h = 0$ and $\alpha = 3\pi/8$ while in Fig. 6(b) we have $\eta_0 = 0$, $d = h = 3\cos(3\pi/8)$ and $\alpha = 3\pi/8$. In both case the curves rotate about the f-axis in an anti clockwise sense contracting to a point in finite time. An animation of the motion of the curve in Fig. 6(b) can be found in [15]. A third type of solution can be constructed by taking the asymptotic behaviour (46) as an initial condition as $\eta \to -\infty$. This again asymptotes to the critical point $R = \sqrt{2},\ f = 0$ as $\eta \to +\infty$. An example of this third type of solution can be found in Fig. 7. Here the curve rotates in a clockwise sense and contracts as it does so.

5.3 *The special cases* $p = 0$

In both the case where we search for an expanding similarity solution of the form

$$r = \sqrt{t}\,R(\theta), \qquad z = \sqrt{t}\,f(\theta),$$

and the case where we search for a contracting similarity solution of the form

$$r = \sqrt{-t}\,R(\theta), \qquad z = \sqrt{-t}\,f(\theta), \tag{49}$$

it is possible to show that

$$\frac{\mathrm{d}^2}{\mathrm{d}\theta^2}\left(\frac{f}{R}\right) + \frac{f}{R} = 0.$$

It follows that f may be expressed in the form

$$f = k\,R\,\cos(\theta + \alpha),$$

where k and α are arbitrary constants, and hence that the solutions are always planar. As such solutions have again been investigated previously in Mullins [9] and Wood [16] we again say no more on the subject, except to note the circular case of (49), namely

$$r = \sqrt{-2t}, \qquad z = 0,$$

which is known [7] to provide the extinction behaviour of closed curves in the planar case and also seems likely to in the three-dimensional case.

6. Discussion

In this work we have investigated the motion of a space curve evolving in accordance to the velocity law $\boldsymbol{v} = \kappa \boldsymbol{n}$. We started by using the Lie group method to classify the symmetries of the partial differential equations describing this evolution. We used the results of this analysis to write down all possible classical similarity reductions to these equations. When we formulated the system in terms of cylindrical polar coordinates r, θ and z (as in equations (10) and (11)), these similarity

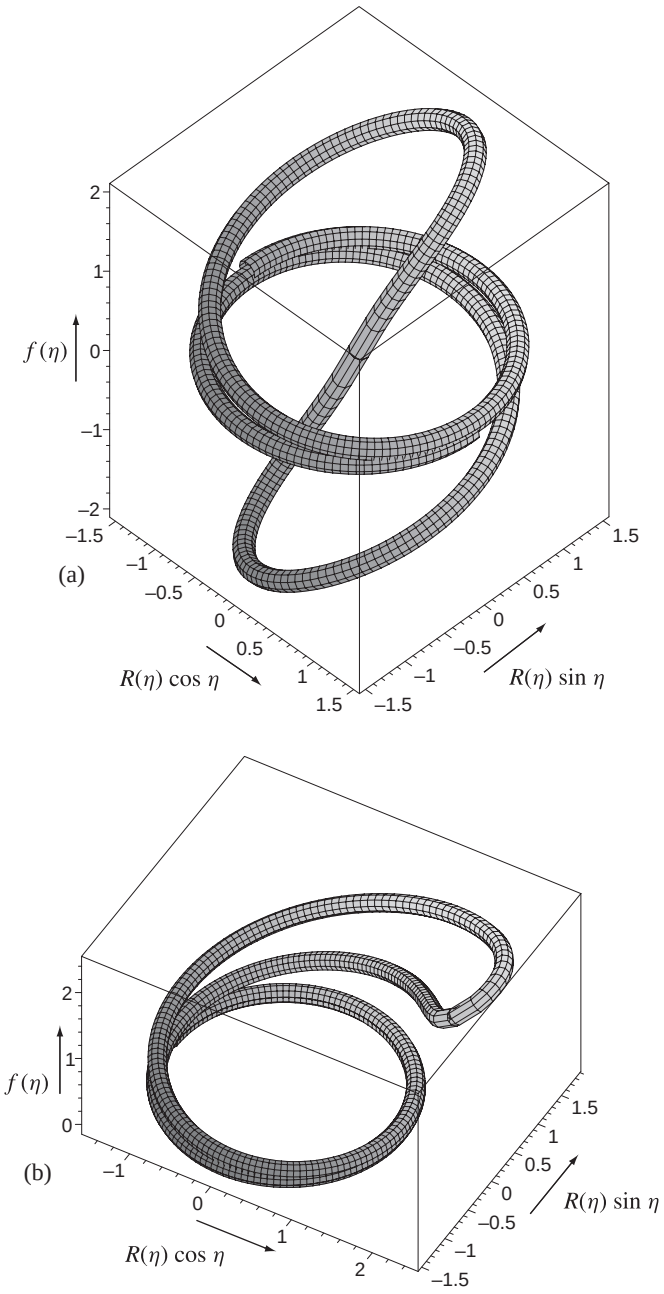

FIG. 6. (a) An example of an antisymmetric contracting logarithmic similarity solution with initial conditions $R \sim \pm\cos(3\pi/8)\sqrt{6\eta}$ and $f \sim \pm\sin(3\pi/8)\sqrt{6\eta}$ as $\eta \to 0$. (b) An asymmetric contracting logarithmic similarity solution with initial conditions $R \sim \cos(3\pi/8)(3 \pm \sqrt{2\eta})$ and $f \sim \sin(3\pi/8)(3 \pm \sqrt{2\eta})$ as $\eta \to 0$. In both cases $p = 1$.

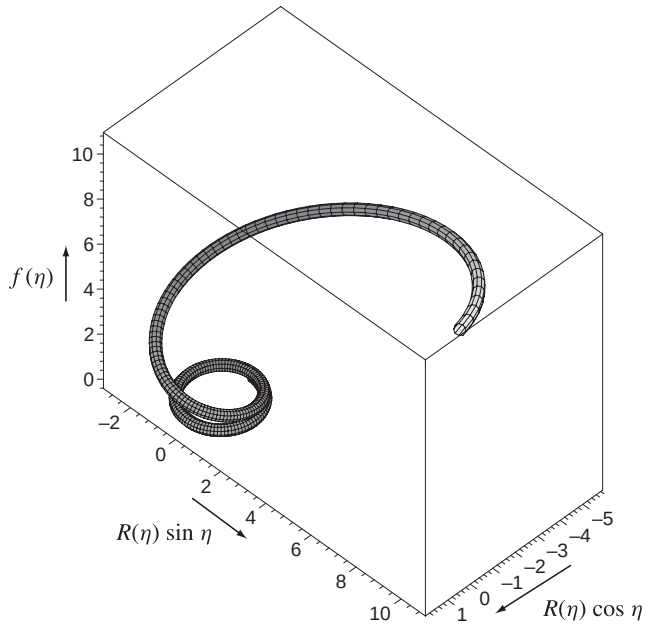

FIG. 7. An example of a contracting similarity solution with the asymptotic behaviour $R \sim \exp(-\eta/(2p))$ and $f \sim \exp(-\eta/(2p))$ as $\eta \to -\infty$. Here $p = 1$.

solutions take the form

$$r = R(\theta - c\,t), \qquad z = q\,t + f(\theta - c\,t), \tag{50}$$

$$r = R(t), \qquad z = k\,\theta + f(t), \tag{51}$$

$$r = \sqrt{t}\,R(\theta - p\log t), \qquad z = \sqrt{t}\,f(\theta - p\log t), \tag{52}$$

$$r = \sqrt{-t}\,R(\theta + p\log(-t)), \quad z = \sqrt{-t}\,f(\theta + p\log(-t)), \tag{53}$$

where c, q, k and p are all arbitrary constants. The similarity form (50) gives rise to rotating travelling waves, special cases of which are rotating waves $q = 0$ and travelling waves $c = 0$. In respect of the travelling wave we were able to show that solutions of this form must be planar. Solutions to (10) and (11) of the form (51) are contracting helices and the similarity forms (52) and (53) we term expanding logarithmic similarity solutions and the contracting logarithmic similarity solutions. The special cases of (52) and (53) in which $p = 0$ give rise to so-called shape preserving solutions; as with the travelling waves, we were able to show that these shape preserving solutions are necessarily planar.

When the model $\boldsymbol{v} = \kappa\boldsymbol{n}$ is used to describe the motion of a line singularity, such as a superconducting vortex or a line disclination, it is useful and interesting to consider the behaviour of the curve where it meets a boundary. The natural boundary condition associated with the law of

motion $\boldsymbol{v} = \kappa \boldsymbol{n}$ is

$$\boldsymbol{t} \wedge \boldsymbol{N} = \boldsymbol{0}, \tag{54}$$

where $\boldsymbol{t}$ is the tangent to curve and $\boldsymbol{N}$ is the normal to boundary. Typically we expect the boundary to be held fixed as the curve evolves. It follows that the only similarity solutions which can be used to describe the motion of a curve which connects to planar boundaries are the shape preserving and travelling wave solutions. It is significant that, as noted above, these are necessarily planar. Such planar shape preserving solutions have been used in [16] to describe the evolution of a curve connected at both ends to a wedge, for example.

It is also of interest to speculate on whether there is any closed curve similarity solution to $\boldsymbol{v} = \kappa \boldsymbol{n}$ other that the obvious contracting circle. It is clear from the catalogue of similarity solutions in (50)–(53) that the only one capable of describing the evolution of a closed curve is (53). Recall that we were unable to find any other behaviour than attraction to the stable critical point at $R = \sqrt{2}$, $f = 0$, as $\eta \to +\infty$ for $p > 0$ and that we could find no evidence of finite η blow-up for increasing η. Furthermore, numerical evidence suggests that, as $\eta \to +\infty$, all trajectories are attracted to this critical point and hence that it is unlikely that closed curve similarity solutions exist other that the obvious one $R = \sqrt{2}$, $f = 0$. However, it is perfectly possible to find long closed curves whose behaviour is approximately described by similarity solutions of the form (53). One has only to think of taking the curve in Fig. 7(b), rotating it by π and joining it back onto its unrotated self somewhere on the plane $f = 0$ with the aid of four judicious cuts and two joins which get rid of the infinite portion of the two curves along the circle $R = \sqrt{2}$, $f = 0$. The resulting finite, but very long, closed curve will follow the evolution of the similarity solution asymptotically, at least until the coils lying along the circle $R = \sqrt{2}$, $f = 0$ are close to unwinding (i.e. have $O(1)$ length in the similarity variables).

Our final comments relate to coupled diffusion equations of the form

$$\begin{aligned} \frac{\partial \alpha}{\partial t} &= \frac{\partial}{\partial z}\left(D_1(\alpha, \beta) \frac{\partial \alpha}{\partial z} \right), \\ \frac{\partial \beta}{\partial t} &= \frac{\partial}{\partial z}\left(D_2(\alpha, \beta) \frac{\partial \beta}{\partial z} \right), \end{aligned} \tag{55}$$

which have a large number of applications. By writing

$$\alpha = \frac{\partial u}{\partial z}, \quad \beta = \frac{\partial v}{\partial z},$$

this system can be re-expressed as

$$\begin{aligned} \frac{\partial u}{\partial t} &= D_1\left(\frac{\partial u}{\partial z}, \frac{\partial v}{\partial z} \right) \frac{\partial^2 u}{\partial z^2}, \\ \frac{\partial v}{\partial t} &= D_2\left(\frac{\partial u}{\partial z}, \frac{\partial v}{\partial z} \right) \frac{\partial^2 v}{\partial z^2}, \end{aligned} \tag{56}$$

and so as an indirect consequence of our analysis we are able to identify the special case

$$D_1(\alpha, \beta) = \frac{1}{1 + \alpha^2 + \beta^2} = D_2(\alpha, \beta), \tag{57}$$

of (55) as having a very rich (albeit non-local) eight-parameter symmetry group; more precisely, two of the rotation groups of (2) correspond to non-local symmetries of (55) with (57) while rotation about the z-axis corresponds to a local symmetry of (55). This result suggests that an analysis of (56) to identify the non-local symmetries of (55) would be highly worthwhile. In particular, we may extend the above result by applying the following geometrical reasoning (or, at the cost of some algebra, by a systematic procedure based on the relevant infinitesimals). For rotation about an axis in the $(u, v, z) = (a, b, c)$ direction it is clear that

$$\frac{a\alpha + b\beta + c}{(1+\alpha^2+\beta^2)^{1/2}},$$

(which is the component of the tangent to the curve in the (a, b, c) direction) is an invariant depending only upon the first derivatives α and β. The angle that the projection of the tangent to the curve onto the plane normal to (a, b, c) makes with the vector $(0, c, -b)$ is

$$\Theta = \tan^{-1}\left(\frac{(b^2+c^2)\alpha - ab\beta - ac}{(a^2+b^2+c^2)^{1/2}(c\beta - b)}\right).$$

Under rotation about (a, b, c) this angle changes by the angle of rotation. Thus

$$\boldsymbol{v} = \mathrm{e}^{\mu\Theta}\Lambda\left(\frac{a\alpha + b\beta + c}{(1+\alpha^2+\beta^2)^{1/2}}\right)\kappa\boldsymbol{n} \tag{58}$$

is invariant under a translation in Θ and a rescaling in time for any function Λ. Formulating this velocity law as a PDE and differentiating with respect to z gives the following system of nonlinear diffusion equations:

$$\begin{aligned}
\frac{\partial\alpha}{\partial t} &= \frac{\partial}{\partial z}\left[\Lambda\left(\frac{a\alpha + b\beta + c}{(1+\alpha^2+\beta^2)^{1/2}}\right)\exp\left(\mu\tan^{-1}\left(\frac{(b^2+c^2)\alpha - ab\beta - ac}{(a^2+b^2+c^2)^{1/2}(c\beta - b)}\right)\right)\right.\\
&\qquad \left.\frac{1}{1+\alpha^2+\beta^2}\frac{\partial\alpha}{\partial z}\right],\\
\frac{\partial\beta}{\partial t} &= \frac{\partial}{\partial z}\left[\Lambda\left(\frac{a\alpha + b\beta + c}{(1+\alpha^2+\beta^2)^{1/2}}\right)\exp\left(\mu\tan^{-1}\left(\frac{(b^2+c^2)\alpha - ab\beta - ac}{(a^2+b^2+c^2)^{1/2}(c\beta - b)}\right)\right)\right.\\
&\qquad \left.\frac{1}{1+\alpha^2+\beta^2}\frac{\partial\beta}{\partial z}\right],
\end{aligned} \tag{59}$$

which inherits as a non-local (unless $a = b = 0$) symmetry the symmetry of (58) under translations of Θ. The corresponding results for the planar case underpin the analysis of [11] (and references therein) though those examples (of scalar nonlinear diffusion equations) have not previously been given the geometrical interpretation

$$\boldsymbol{v} = \mathrm{e}^{\mu\Theta}\kappa\boldsymbol{n}, \tag{60}$$

in two dimensions with $\Theta = \tan^{-1}(\partial u/\partial z)$. Equation (60) implies that

$$\frac{\partial\alpha}{\partial t} = \frac{\partial}{\partial z}\left(\frac{\mathrm{e}^{\mu\tan^{-1}\alpha}}{1+\alpha^2}\frac{\partial\alpha}{\partial z}\right),$$

so setting $\mu = -2in$, $\alpha = ic$ is often expedient, leading to

$$\frac{\partial c}{\partial t} = \frac{\partial}{\partial z}\left(\frac{(1+c)^{n-1}}{(1-c)^{n+1}}\frac{\partial c}{\partial z}\right).$$

Having μ and α imaginary obscures the geometrical derivation and content, however.

Finally, it is worth noting the similarity of such results to λ–ω reaction diffusion systems. For $a = b = 0$, the relevant symmetry of (58) is a local one. For $a = b = \mu = 0$, (59) takes the form

$$\frac{\partial \gamma}{\partial t} = \frac{\partial}{\partial z}\left(D(|\gamma|)\frac{\partial \gamma}{\partial x}\right) \tag{61}$$

with $\gamma = \alpha + i\beta$; (61) is evidently invariant under $\gamma \to \gamma e^{i\phi}$ for constant ϕ, and the result represents a nonlinearly diffusive version of that for the λ–ω reaction diffusion systems, readily generalizing to

$$\frac{\partial \gamma}{\partial t} = \frac{\partial}{\partial z}\left(D(|\gamma|)\frac{\partial \gamma}{\partial x}\right) + (\lambda(|\gamma|) + i\omega(|\gamma|))\,\gamma, \tag{62}$$

for example. Systems such as (62) thus warrant further attention.

Acknowledgements

GR gratefully acknowledges the support of a Leverhulme Special Research Fellowship.

REFERENCES

1. ALTSCHULER, S. J. Singularities of the curve shrinking flow for space curves. *J. Diff. Geom.* **34**, (1991) 491–514.
2. ALTSCHULER, S. J. & GRAYSON, M. A. Shortening space curves and flow through singularities. *J. Diff. Geom.* **35**, (1992) 283–298.
3. SPECIAL ISSUE Vortices, dislocations and line singularities in partial differential equations. *Phil. Trans. Roy. Soc. Lond. Ser.* A **355**, (1997) 1945–2072.
4. AMBROSIO, L. & SONER, H. M. Level set approach to mean curvature flow in arbitrary codimension. *J. Diff. Geom.* **43**, (1996) 693–737.
5. CALLEGARI, A. J. & TING, L. Motion of a curved vortex filament with decaying vortical core and axial velocity. *SIAM J. Appl. Math.* **35**, (1978) 148–175.
6. CHAPMAN, S. J. & RICHARDSON, G. Motion of vortices in type-II superconductors. *SIAM J. Appl. Math.* **55**, (1995) 1275–1296.
7. GAGE, M. E. Curve shortening makes convex curves circular. *Invent. Math.* **76**, (1984) 357–364.
8. KEENER, J. P. & TYSON, J. J. The dynamics of scroll waves in excitable media. *SIAM J. Appl. Math.* **34**, (1992) 1–39.
9. MULLINS, W. W. Two-dimensional motion of idealised grain boundaries. *J. Appl. Physics* **27**, (1956) 900–904.
10. HYDON, P. E. *Symmetry methods for differential equations*. Cambridge University Press, Cambridge (2000).
11. KING, J. R. Exact solutions to some nonlinear diffusion equations. *Quart. J. Mech. Appl. Math.* **42**, (1989) 537–552.

12. LIN, T. Rigorous and generalised derivation of vortex line dynamics in superfluids and superconductors. *SIAM J. Appl. Math.* **60**, (2000) 1099–1110.
13. MOORE, D. W. & SAFFMAN, P. G. The motion of a vortex filament with axial flow. *Phil. Trans. Roy. Soc. Lond. Ser.* A **272**, (1972) 403–429.
14. RICHARDSON, G. Line disclination dynamics in uniaxial nematic liquid crystals. *Quart. J. Mech. Appl. Math.* **53**, (2000) 49–71.
15. RICHARDSON, G. http://www.maths.nottingham.ac.uk/personal/etzgwr/simcurv.html. (2000).
16. WOOD, G. P. Some problems in nonlinear diffusion, Ph.D. Thesis, University of Nottingham, (1996).